Prevalence and mechanisms of high-level carbapenem antibiotic tolerance in clinical isolates of *Klebsiella pneumoniae*

Authors: Trevor Cross[1,2], Facundo Torres[1,2], Abigail P. McGee[2*], Tolani Aliyu[2], Lars F. Westblade[3], Abhyudai Singh[4], Tobias Dörr[1,2,5]

[1]Department of Microbiology, Cornell University, Ithaca, NY

[2]Weill Institute for Cell and Molecular Biology, Cornell University, Ithaca, NY

[3] Departments of Pathology and Laboratory Medicine, Medicine, and Pediatrics, Weill Cornell Medicine, New York, NY

[4] Department of Electrical and Computer Engineering, University of Delaware, Newark, DE, 19716, USA

[5] Cornell Institute for Host-Microbe Interactions and Disease (CIHMID)

[*]Current affiliation: Graduate Program in Microbiology and Immunology, Geisel School of Medicine, Dartmouth

Keywords: meropenem, cell envelope stress response, spheroplast, L-form, MltB

Abstract:

Antibiotic tolerance is the ability of bacteria to survive normally lethal doses of antibiotics for extended time periods. Clinically significant Enterobacterales, for example, often exhibit high tolerance to the last-resort antibiotic meropenem. Meropenem tolerance is associated with formation of cell wall-deficient spheroplasts that readily recover to rod shape and normal growth upon removal of the antibiotic. Both the true prevalence of tolerance, and genetic mechanisms underlying it, remain poorly understood. Here, we find that meropenem tolerance is widespread among clinical Enterobacterales. Using forward genetics, we uncover novel tolerance factors in a hypertolerant isolate of the

ESKAPE pathogen *Klebsiella pneumoniae*. We find that multiple mechanisms contribute to tolerance, and that cell envelope stress responses (PhoPQ, Cpx, Rcs and OmpR/EnvZ) collectively promote spheroplast stability and recovery, while the lytic transglycosylase MltB counteracts it. Our data indicate that tolerance is widespread among clinical isolates, and that outer membrane maintenance is a key factor promoting survival of tolerant *K. pneumoniae.*

Introduction

Healthcare-associated infections are common sequelae of hospitalization and increasingly, treatment of these infections fails due to antibiotic resistance [1]. However, treatment also often fails despite the absence of outright resistance [2]. This has been attributed to other strategies bacteria have for evading complete eradication, including the well-characterized phenomenon of bacterial persistence [3]. However, between the extremes of frank resistance and persistence there is considerable complexity in bacterial antibiotic susceptibility patterns. For example, antibiotic tolerance, which has recently received increased attention as another means of surviving antibiotic insult, represents a state where a large fraction of a susceptible bacterial population survives in the presence of an antibiotic for extended periods. Gram-negative bacteria in particular can enter a non-replicative, cell wall-deficient spheroplast form upon treatment with β-lactam antibiotics [4-7]. This phenotype is reminiscent of L-forms [8-10] with the distinction that spheroplasts (unlike L-forms) do not proliferate in the presence of antibiotic. Spheroplasts remain intact for extended time periods and readily recover their cell shape and resume

46 division when the β-lactam drug is removed. However, the true prevalence of β-lactam
47 tolerant Gram-negative pathogens among clinical isolates is unknown.

48 *Klebsiella pneumoniae* is a Gram-negative nosocomial pathogen that can cause a
49 variety of opportunistic infections, including eponymous pneumonia, bloodstream
50 infections and UTIs [11]. A member of the infamous ESKAPE group of pathogens, *K.*
51 *pneumoniae* exhibits particularly worrisome levels of treatment failure [12]. Due to the
52 high level of resistance against most β-lactams, the carbapenems remain one of the
53 leading antibiotic classes that are effective against *K. pneumoniae* [13]. Determining
54 mechanisms that alter susceptibility against β-lactams in general, and carbapenems in
55 particular, is thus a critical need for developing new treatment options against *K.*
56 *pneumoniae.*

57 β-lactams covalently and irreversibly bind to so-called penicillin-binding proteins
58 (PBPs), which are the principal synthases of the main cell wall component peptidoglycan
59 (PG). β-lactam binding results in several downstream events that contribute to cell death
60 in poorly-defined ways [14]. Endogenous cell wall lytic enzymes (collectively referred to
61 as autolysins) degrade the PG sacculus into monomers and ultimately eliminate the
62 sacculus entirely. In some bacteria, cell wall degradation can cause catastrophic rupture
63 and cell lysis, for example in the well-studied model organism *E. coli.* In addition, the
64 constant synthesis and immediate autolysin-mediated degradation of PG (futile cycling)
65 depletes cellular resources, exacerbating detrimental effects independent of cell lysis [15,
66 16]. Interestingly, β-lactam exposure coincides with the generation of damaging reactive
67 oxygen species (ROS), though the contribution of ROS to β-lactam killing is not entirely
68 clear [17]. It is thought that the combination of these direct and indirect effects likely

collectively contributes to cell death by lysis or internal damage. How tolerant cells manage this assault to stay alive has remained poorly understood, but previous work has implicated cell envelope stress signaling in spheroplast survival [17-19]. In the cholera pathogen *Vibrio cholerae*, for example, the VxrAB system is induced by β-lactam stress, resulting in the upregulation of cell wall synthesis functions (which readies the cell for recovery once the antibiotic is removed) and downregulation of detrimental iron influx (putatively to reduce the damage sustained by ROS production) [17].

In this study, we sought to characterize meropenem tolerance in *K. pneumoniae*. We found that clinical isolates of this nosocomial Gram-negative pathogen often exhibit high levels of meropenem tolerance. Using TnSeq, we defined genetic requirements for tolerance, and uncovered a role for cell envelope stress signaling systems in both spheroplast maintenance and recovery. Our data open the door for a more in-depth understanding of the molecular mechanisms promoting tolerance, priming the future design of antibiotic adjuvants that eradicate tolerant cells.

Results

Klebsiella species clinical isolates exhibit high meropenem tolerance

As part of a larger effort to determine the role of antibiotic tolerance in healthcare settings, we characterized a large panel of bloodstream isolates from the culture collection of Weill Cornell Medical (WCM). This de-identified 271 isolate panel (Table S1) is fully characterized through antimicrobial susceptibility testing and consists of a large number

of mostly carbapenem-susceptible (MIC <1 μg/mL) Gram-negative pathogens, with three isolates testing as intermediate (MIC = 2) and seven strains as fully resistant (MIC > 4 μg/mL; one strain due to its possession of the KPC carbapenemase). Since the majority of the isolates are carbapenem susceptible, we considered this an ideal panel for determination of how prevalent carbapenem tolerance (rather than resistance) is in clinical samples. Currently, no fully-established sufficiently high throughput tolerance assay exists [20], and we therefore chose to use a semi-quantitative assay for our screen. To this end, we grew the isolate panel (curated to remove the resistant isolates with MIC > 4 μg/mL) in a 96-well format, where we exposed cells to meropenem (10 μg/mL, 5x – 100x MIC) at high cell densities (following a 10-fold dilution of overnight culture into fresh medium). At an eight-hour timepoint, 5 μL of thus-treated cultures were then spotted on an agar plate together with 5 ng of purified carbapenemase (KPC-2) to remove the antibiotic. After 24 hours of incubation, spots were then scored as full growth (a confluent spot = high tolerance), growth with a few visible colonies (= intermediate) or no growth (= low tolerance) (**Fig. 1A, S1**). Since this panel contained isolates exhibiting a wide distribution of susceptibilities to meropenem (MICs ranging from ≤0.015 – 4 μg/mL), we considered the possibility that apparent differences in tolerance may instead indicate differences in MIC. Plotting tolerance categories over MIC values revealed that all 3 tolerance categories contained isolates with similar variance in MICs (**Fig. 1B**). As an example, all isolates in **Fig. 1A** with a yellow circle had comparatively high MICs (>1 μg/mL), but displayed very different survival levels at 8 and 24 hours of meropenem exposure. Thus, tolerance as determined in this assay is not a simple function of MIC variation; rather, these data suggest that our assay captures true tolerance.

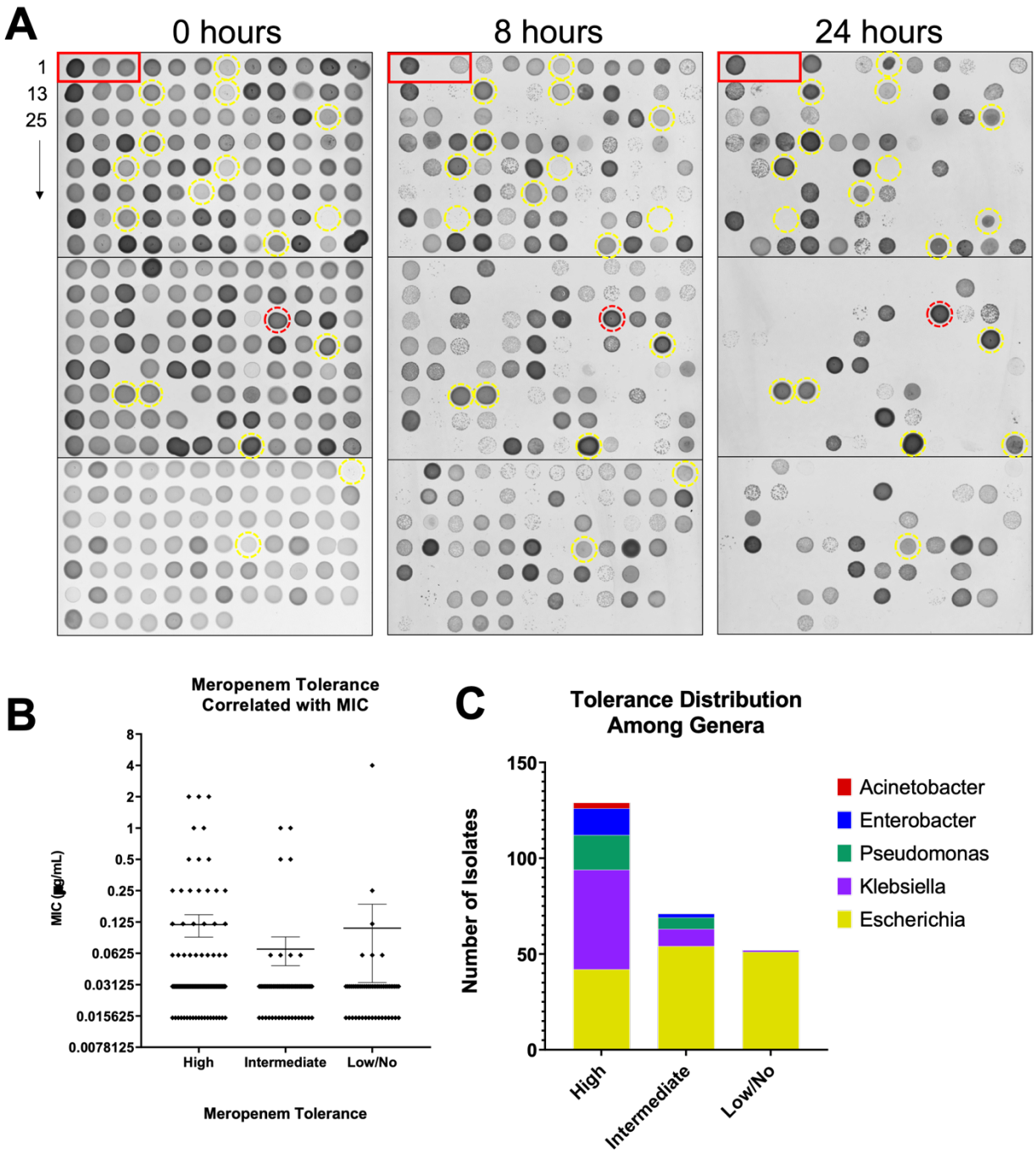

Figure 1: Widespread meropenem tolerance among bloodstream isolates

(A) A panel of bloodstream isolates was exposed to 10 µg/mL (>2x MIC for all isolates) meropenem in 96-well format (BHI medium) and incubated for 8 hours or 24 hours. Following incubation, purified KPC-2 enzyme was added to the wells, and 10 µL transferred to a BHI plate without antibiotic. Tolerance was scored qualitatively as the ability to form colonies/confluent growth after 8 or 24 hours. Yellow circles indicate examples of different tolerance levels across high MIC (>/=1 µg/mL). Red circle indicates

the positive control (resistant KPC+ strain). Red box indicates examples of (from left to right) a highly tolerant *Klebsiella pneumoniae* isolate, a medium tolerant *E. coli* and a low tolerance *E. coli.* (B) Tolerance categories were plotted with their corresponding MIC values. (C) Genus distribution among the tolerance categories.

We then asked whether some genera were more likely to display tolerance than others, and to this end plotted tolerance as a function of bacterial genus. Interestingly, the low tolerance fraction was almost exclusively occupied by *E. coli* isolates (consistent with our previous observations [7]), while the high tolerance fraction was enriched in *Enterobacter species., Pseudomonas aeruginosa*, and especially *Klebsiella pneumoniae* (**Fig. 1C**). Thus, *K. pneumoniae* clinical isolates are particularly likely to display antibiotic tolerance among clinical isolates of Enterobacterales.

The K. pneumoniae TS1 isolate is highly meropenem tolerant

Since *K. pneumoniae* clinical isolates answered our survey as particularly tolerant, we chose to focus on this species for further study of meropenem tolerance. However, we noted that different *K. pneumoniae* isolates diverged in tolerance levels in our spot assay (**Fig. 1A**). To more quantitatively determine strain-specific differences, and to identify new model strains for mechanistic studies, we compared two well-characterized clinical isolates of *K. pneumoniae* for their tolerance levels *in vitro*, namely *K. pneumoniae* strains TS1 (a derivative of the CDC isolate bank AR0080) and KPNIH1 [21]. Both strains have been cured of their carbapenemase-containing plasmids and are thus fully meropenem susceptible (**Table S2** MICs). Time-dependent killing experiments in the

145 presence of 10 µg/mL meropenem revealed drastic differences in tolerance levels
146 between the two strains, despite their similarly low MICs (**Fig. 2, Table S2**).

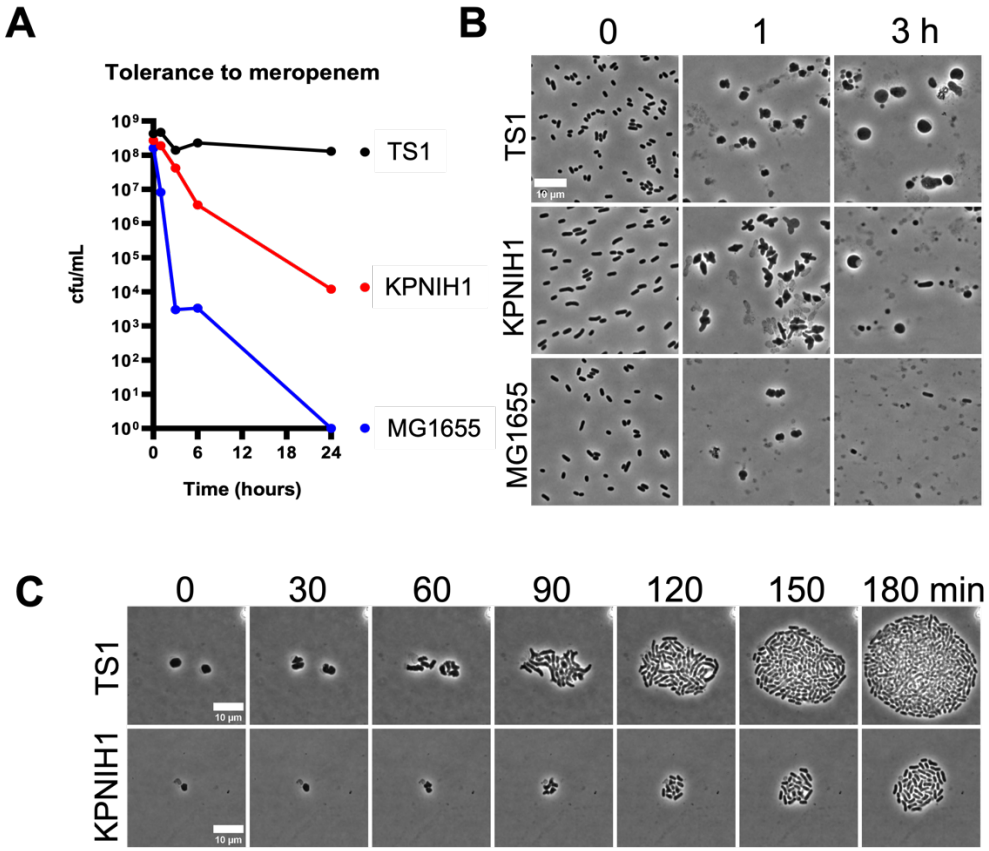

147

148 **Figure 2: *K. pneumoniae* TS1 is a hypertolerant clinical isolate**

149 (A) Example time-dependent killing experiment (BHI medium) in meropenem (10 µg/mL)
150 reveals differences in tolerance levels among two *K. pneumoniae* isolates (with the model
151 *E. coli* strain MG1655 as comparison). (B) Tolerance in *K. pneumoniae* is associated with
152 spheroplast formation. Aliquots from the experiment depicted in panel (A) were
153 transferred to agarose slides at the indicated time-points and imaged. (C) Recovery after
154 addition of purified KPC-2 carbapenemase demonstrates spheroplast viability.

155

156 This observation supports our previous finding of widely different tolerance levels
157 between different isolates of the same species [7]. Both *K. pneumoniae* strains still
158 exhibited higher levels of survival relative to the low-tolerance *E. coli* MG1655 comparison

strain, which exhibited a steep, 4.5 log reduction in viability within six hours of meropenem treatment, and complete elimination by 24 hours of exposure. The TS1 strain was almost completely tolerant, with only a slight (5-10 fold) decrease in viability even after 24 hours of exposure (**Fig. 2A**). In contrast, the KPNIH1 isolate drastically lost viability by 10,000-fold after 24 hours. In *both Klebsiella* isolates, survival coincided with formation of cell wall-deficient spheroplasts (**Fig. 2B**) that readily recovered to rod-shape morphology upon removal of the antibiotic (**Fig. 2C**). We also used these three benchmark strains to validate our high-tolerance spot assay (**Fig. 1A**). Consistent with the time-dependent killing experiments (**Fig. 2A**), TS1 scored as highly tolerant, KPNIH1 as intermediate, and MG1655 as non-tolerant in the spot assay (**Fig. S1**). Thus, the TS1 isolate is highly meropenem tolerant, and serves as an ideal model for a mechanistic characterization of spheroplast formation and recovery.

A TnSeq approach reveals putative tolerance genes in K. pneumoniae TS1

We next sought to identify factors that contribute to meropenem tolerance in *K. pneumoniae*. To this end, we conducted a transposon-insertion sequencing screen to assemble a genome-wide mutant fitness map in the presence of meropenem and compared insertion frequencies before and after 6 hours of meropenem challenge (including an outgrowth step, see methods for details, **Fig. 3A**).

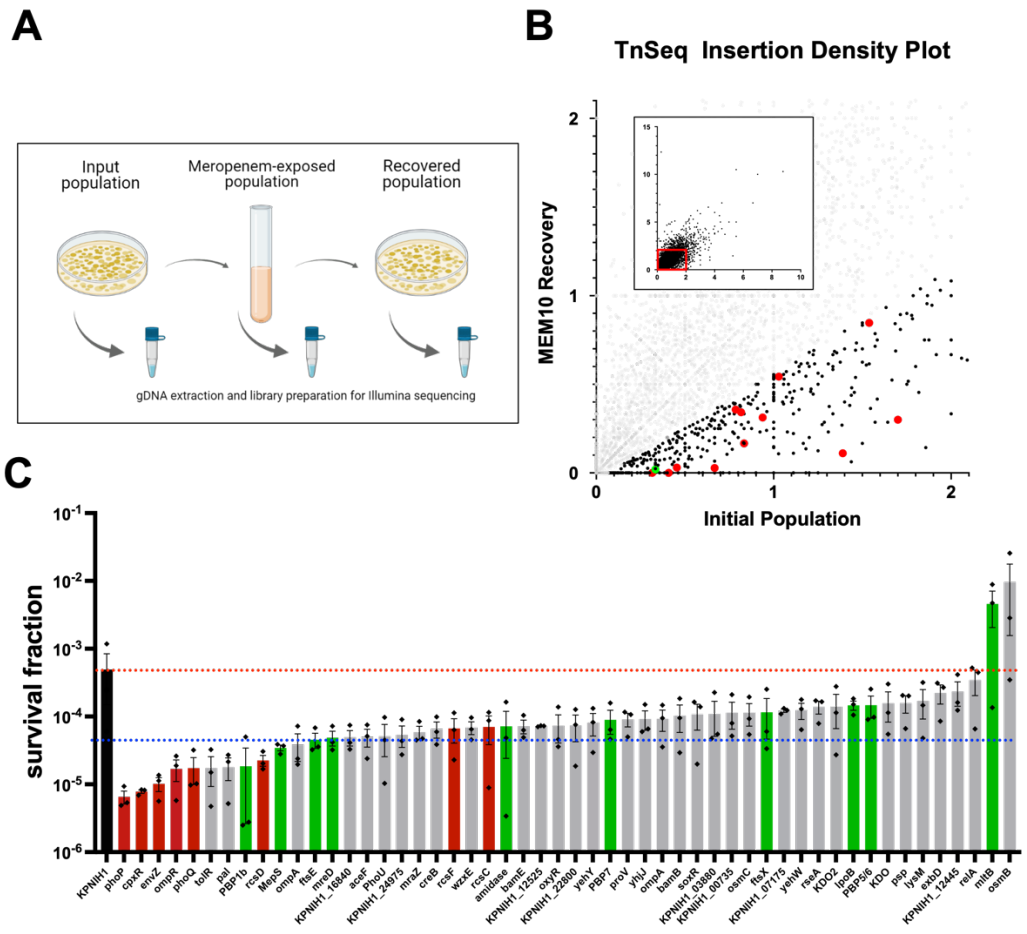

Figure 3: TnSeq identifies genetic determinants of meropenem tolerance.

(A) Outline of TnSeq experimental procedure. (B) Identification of significant candidate tolerance factors in TS1 by plotting insertion density of a recovered library vs. the input library. (C) Validation of TnSeq hits. Mutants were obtained from the KPNIH1 mutant library and exposed to meropenem (10 µg/mL) for 6 hours, followed by dilution and spot-plating. Raw data of 3 independent biological replicates are shown +/- standard deviation. Red dotted line indicates WT average survival level; blue dotted line represents the 10fold reduced survival benchmark.

The screen uncovered many expected and novel putative tolerance genes (**Fig. 3B**). Notably, the gene coding for PBP1b was detected within the top two percent of candidate essential genes for tolerance to meropenem. Class aPBPs like aPBP1b have an established role in rebuilding the cell wall after damage [22, 23], and thus serve as

192 internal validation of our screening conditions, establishing confidence in our screening
193 approach. Next, we validated our most prominent (top 10%) hits. We used an ordered,
194 commercially available transposon insertion library in the intermediate tolerance strain
195 KPNIH1 [21] for a first-pass validation. This resulted in confirmation of several genes
196 whose inactivation either promoted or decreased tolerance (**Fig. 3C**). The reduced
197 tolerance fraction was enriched in cell envelope functions (**Fig. 3C**, green bars), which is
198 expected due to the need to re-establish a cell wall upon spheroplast recovery. We also
199 noticed that disruptions in several cell envelope stress response systems (*rcs*, *pho*, *cpx*,
200 and *ompR-envZ*), drastically reduced survival during meropenem stress (**Fig. 3C**, red
201 bars), while two gene disruptions (in the gene for the cell wall lytic enzyme MltB, and in
202 the poorly characterized outer membrane lipoprotein OsmB), increased survival. Taken
203 together, these results demonstrate that the *K. pneumoniae* TnSeq experiment was
204 effective at identifying specific genes with roles in meropenem tolerance, lending
205 themselves to further study as outlined below.

206

207 *The lytic transglycosylase* MltB *endogenously reduces meropenem tolerance*

208 Our TnSeq screen identified both genes that promote meropenem tolerance as
209 well as genes which endogenously reduce tolerance. The gene coding for the lytic
210 transglycosylase enzyme MltB, for example, answered the screen as imparting a severe
211 fitness cost in the presence of meropenem. This was unexpected, since bacteria have
212 many functionally redundant lytic transglycosylase paralogs throughout their genomes,
213 and phenotypes associated with a single deletion are thus rare [24]. To dissect the role
214 of LTGs in meropenem tolerance further, we tested a panel of transposon disruption

mutants in known and predicted LTG genes for meropenem tolerance in the lower tolerance strain KPNIH1. Among eleven mutants tested, only *mltB::tn* and (to a lesser degree) *sltY::tn* exhibited significantly increased survival in the presence of meropenem, with a drastic 1000-fold increase in survival after 24 hours for *mltB* and 100-fold for *sltY* (**Fig. 4A**). Time-dependent killing experiments confirmed a strong role for MltB as an antagonist of antibiotic tolerance, as the *mltB::tn* mutant exhibited minimal (5-fold) killing in the presence of meropenem over 24 hours (**Fig. 4B**).

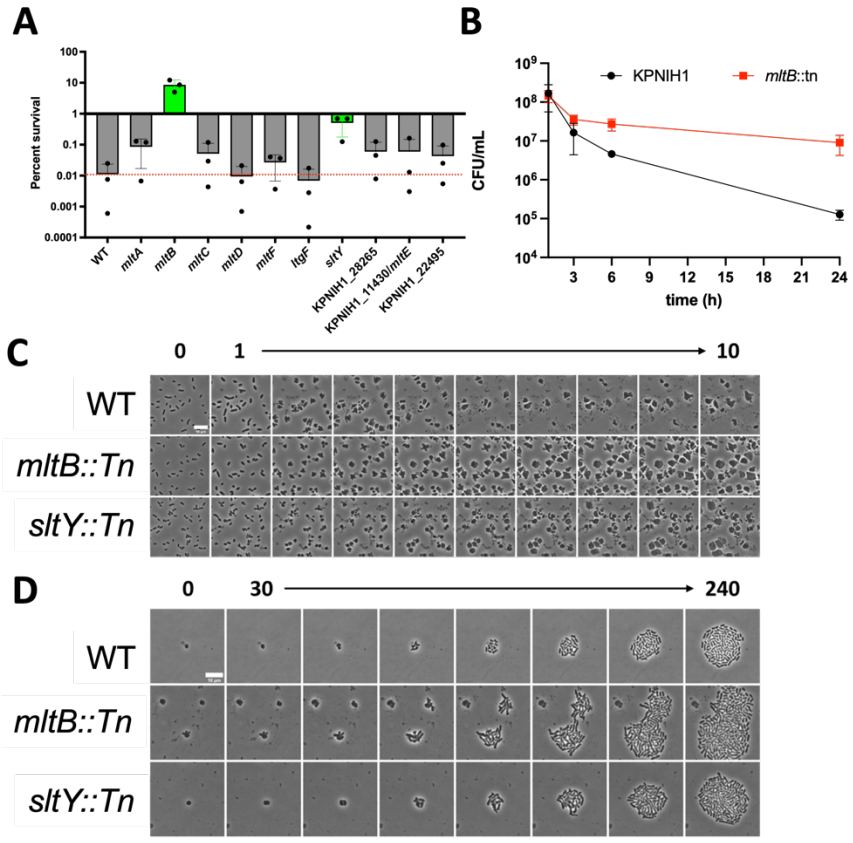

Figure 4: mltB and sltY reduce tolerance to meropenem and prevent cells from retaining polar morphology

(A) Survival of mutants in lytic transglycosylases. Mutants were obtained from the KPNIH1 mutant library and exposed to meropenem (10 µg/mL) for 6 hours, followed by dilution and spot-plating. (B) Time-dependent killing reveals increased tolerance in an *mltB* mutant. (C) Cell wall degradation in LTG mutants. Bacteria were applied to an

agarose pad containing BHI and 10 µg/mL meropenem. Images were taken every hour. (D) Recovery dynamics of spheroplasts. Cells were treated with meropenem (10 µg/mL) for 6 hours. Purified KPC-2 was then added, followed by timelapse microscopy.

The *mltB::tn* and *sltY:tn* mutants were further characterized by examining cell morphology upon spheroplast formation and recovery. Timelapse microscopy of cells exposed to meropenem revealed that the *mltB::tn* and *sltY:tn* disruption mutants retained morphology at the cell poles for longer than the wild type parent strain, and qualitatively exhibited an increase in the relative abundance of intact spheroplasts (**Fig. 4C**); this coincided with qualitatively enhanced recovery dynamics (**Fig. 4D**). These data suggest that *mltB* and (to a lesser extent) *sltY* reduce tolerance by accelerating the degradation of peptidoglycan when synthesis is halted by meropenem, and thus point to a dominant role of these LTGs in cell wall turnover in *K. pneumoniae*. These data suggest that activation of autolysins could be a useful future strategy to potentiate β-lactam antibiotics against tolerant pathogens.

Multiple cell envelope stress responses systems collectively contribute to β-lactam tolerance

Several well-characterized cell envelope stress response systems appeared in our screen as top candidates that promote meropenem tolerance: the Rcs phosphorelay system, the PhoPQ and CpxAR two-component systems, and the osmotic and acid stress response system, OmpR/EnvZ. Of note, our previous study revealed the PhoPQ system as a key meropenem tolerance determinant in *Enterobacter cloacae,* suggesting that PhoPQ may be a widely conserved tolerance determinant [25]. To dissect the individual

and combined contributions of these systems to survival in meropenem, we created deletions of all four systems in all combinations, including one quadruple system deletion mutant lacking all four stress responses. These mutants were then exposed to meropenem in time-dependent killing assays. These experiments revealed a 10 to 10,000-fold decrease in viability after 24 hours of exposure to meropenem in any individual envelope stress response mutant compared to the wild type *K. pneumoniae* parent strain (**Fig. 5AB**). We observed large differences in both magnitude and consequences for lysis in the different mutants. The Δ*ompR/envZ* mutant, for example, exhibited the most drastic reduction in viability of all the single mutants (10,000-fold vs. 10- to 100-fold for the others), pointing to a particularly important role of the OmpR/EnvZ response in tolerance to meropenem. We also noticed that while most single mutants exhibited both a drop in cfu/mL and in OD_{600} (indicative of cell lysis), the Δ*rcsF* mutant was only defective in viability, but increased in OD during meropenem treatment, suggesting a role for Rcs in spheroplast recovery, rather than structural maintenance.

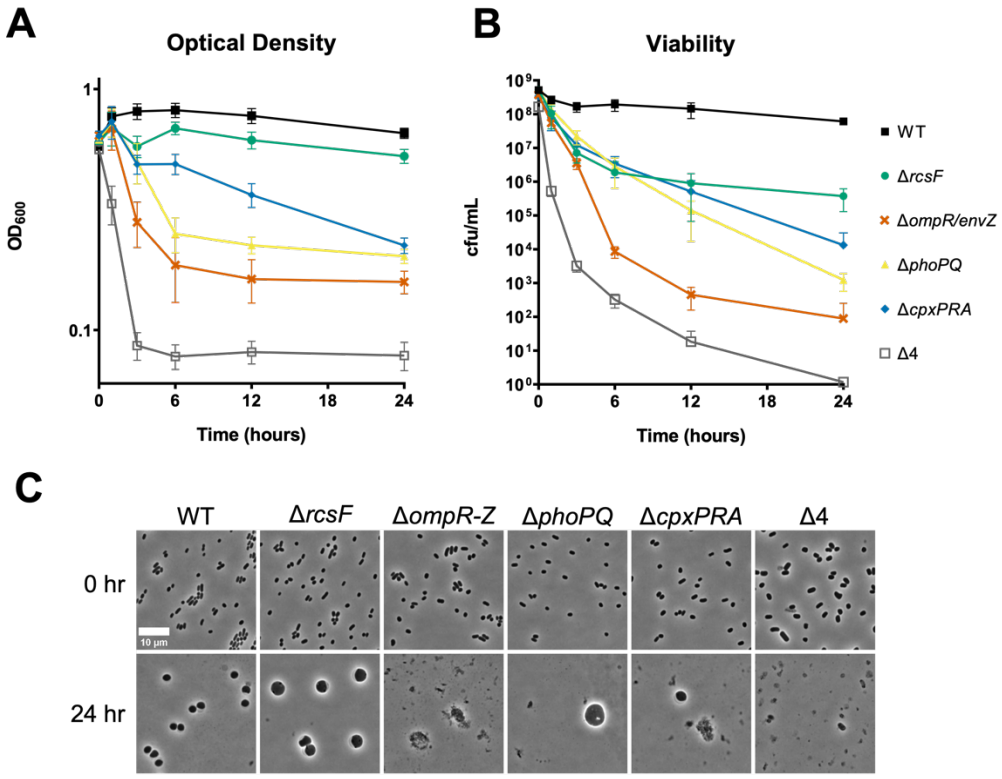

Figure 5: Cell envelope stress response systems are essential for full meropenem tolerance

Cells were diluted 10fold into 5 mL of BHI medium containing 10 µg/mL meropenem. At the indicated timepoints, samples were withdrawn and OD_{600} (A) and CFU/mL (B) were measured. (C) Aliquots were removed from the experiment depicted in (A-B) and imaged.

We also investigated cell morphologies of each mutant before and after exposure to meropenem for 24 hours of treatment, and upon recovery in strains capable of forming spheroplasts. Wild type cells and all single deletion mutants appeared similar in shape and morphology at the start of meropenem exposure experiments (**Fig. 5C**). However, the Δ4 mutant cells exhibited slightly aberrant morphology (slightly larger cells with subtle deformations) and spontaneous lysis, suggested by the presence of cell debris. After 24 hours of meropenem exposure, most single deletion mutants (with the exception of Δ*ompR/envZ*) formed spheroplasts with no clear difference in structure compared to the

wild type, albeit a much lower numbers (consistent with the decrease in OD_{600}). Qualitatively, the microscopy analysis confirmed that the Rcs system does not appear to be essential for structural maintenance of spheroplasts, as the Δ*rcsF* mutant showed little evidence of lysis, and wild-type levels of spheroplasts (**Fig. 5C**). Thus, the Rcs system may play a role in spheroplast recovery, rather than spheroplast cell envelope maintenance, consistent with a role in spheroplast recovery in lysozyme-treated *E. coli* [26]. Interestingly, the Δ*ompR/envZ* and Δ4 mutants were highly defective in spheroplast formation or maintenance, as we failed to find any intact spheroplasts even upon 10-fold concentration of meropenem-treated culture followed by imaging, consistent with the drastic reduction in viability these strains experience in the presence of meropenem (**Fig. 5B**). We also constructed intermediate strains, including a suite of Δ3s with single two-component systems left intact (**Fig. S3**). Interestingly, all Δ3s collapsed in viability almost to the same degree as the Δ4, strongly suggesting an additive or synergistic effect between the different systems, as no two-component system by itself could sustain viability. Of note, among the Δ2 mutants, the combination of Δ*ompR/envZ* and Δ*rcs* was most detrimental, and the resulting mutant was, like the Δ4 mutant, nearly eradicated after 24 hours of exposure. Collectively, these results point to a hierarchical organization of responses necessary for meropenem tolerance; OmpR/EnvZ as the primary response, followed by Pho and Cpx to maintain spheroplast stability, and Rcs to aid in recovery.

The Rcs phosphorelay is induced by, and required for, meropenem tolerance

The Rcs phosphorelay as an apparent contributor to tolerance caught our attention. In *E. coli*, Rcs is induced by β-lactams, and required for survival in low β-lactam concentrations

[27]. Additionally, Rcs is required for recovery of *E. coli* from a cell wall-deficient state (generated by lysozyme treatment in osmostabilized medium, a condition that morphologically mimics meropenem-treated spheroplasts) [26]. In apparent contrast, a recent study has shown that Rcs is neither induced by, nor required for β-lactam persisters [28]; however, this is likely because persisters are dormant and thus not expected to be damaged by the antibiotic (obviating the need for a damage response) [3]. To clarify the role of Rcs in *K. pneumoniae*, we engineered a TS1 strain carrying an P_{rprA}-*lacZ* transcriptional fusion (a well-established readout of Rcs signaling [29]) in a neutral chromosomal locus (*lacZ*) and measured induction by meropenem. A first qualitative assay using zone of inhibition on growth medium containing the chromogenic LacZ substrate X-gal yielded a blue ring around the zone of inhibition when a meropenem disk was placed on the agar surface, but not when the translation inhibitor kanamycin was used (**Fig. S4A**). We then corroborated these results in liquid medium, where a quantitative β-galactosidase activity assay (Miller assay) revealed strong (30fold), time-dependent induction of the construct by meropenem (**Fig. 6A**). Thus, meropenem induces the Rcs response. We also validated the role of Rcs in meropenem tolerance by creating additional mutants in Rcs components, namely RcsF, RcsC and RcsD. All mutants displayed a strong (10,000fold) reduction in tolerance, which could be fully complemented by overexpression of the response regulator RcsB (**Fig. 6B**). The ability of RcsB overexpression to induce the Rcs regulon was verified by measuring induction of the chromosomal P_{rprA}-*lacZ* construct (**Fig. S4B**). Thus, the Rcs phosphorelay is both responsive to meropenem exposure, and required for meropenem tolerance in *K. pneumoniae.*

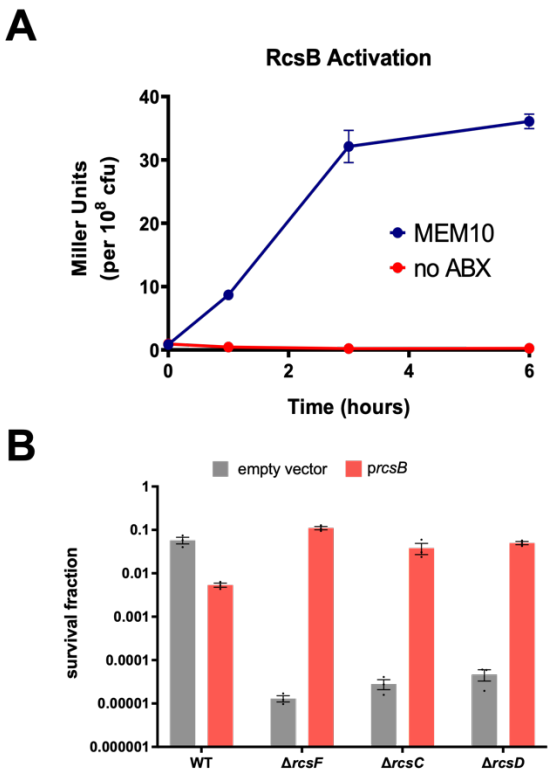

Figure 6: The Rcs phosphorelay is induced by meropenem and required for tolerance

(A) A strain carrying a chromosomal rprA-*lacZ* transcriptional fusion was exposed to meropenem, followed by quantification of beta-galactosidase activity via Miller assay (B) The indicated strains were exposed to meropenem (10 µg/mL). Survival fraction is CFU/mL after 24 hours normalized to starting cell density. Shown are averages of 3 independent experiments +/- standard error.

Fluctuation test reveals memory in tolerant subpopulation

The stress responses that contribute to meropenem tolerance may rely on deterministic induction by the antibiotic for their protective impact, or they may be stochastically and heterogeneously active within the population before exposure to a stress as a bet-hedging strategy. To gain some insight into this distinction, we leveraged the classical Luria-Delbrück experiment or the “Fluctuation Test” that has been recently expanded to

investigate reversible switching between cellular states within an isogenic cell population. This fluctuation test has been used to gain insights into the non-genetic mechanisms by which microbial and cancer cells survive lethal exposures to targeted drug therapy [30-32]. For example, the application of the fluctuation test in both *Escherichia coli* [33] and *Bacillus megaterium* [34] has shown individual cells to reversibly switch between an antibiotic-sensitive and an antibiotic-tolerant state, with each state being maintained transiently for several generations. This reversible switching happens continuously in the absence of the drug as a result of stochastic fluctuations in underlying signaling and gene regulatory networks and primes a rare subpopulation of cells as a bet-hedging mechanism to survive lethal antibiotic exposure.

To conduct a fluctuation test, we first isolated single TS1 cells in 96-well plates using serial dilution. Each cell was grown into a clonal population and exposed to meropenem at an OD_{600} of 0.3 (**Fig. 7**). WT OD dropped sharply at first, followed by slower increase in OD_{600} in the surviving subpopulation (spheroplasts). The clone-to-clone fluctuations in cell viability after antibiotic exposure were quantified by using the coefficient of variation (standard deviation divided by the mean) of OD_{600} (spheroplast survivor fraction) across clones at 1.66 hours after drug exposure. This time point was specifically chosen as it captures the OD_{600} drop-off in response to meropenem and avoids the rebound in OD_{600} seen in WT cells as a result of changes in cell shape. We then used mathematical modeling to predict how the kinetics of switching between drug-sensitive and drug-tolerant cell states impact clone-to-clone fluctuations in the number of cells surviving lethal stress, with slower switching (i.e., higher transient memory of a state being retained across generation) resulting in a higher degree of interconal fluctuations

366 [32]. Our results show clone-to-clone fluctuations in cell integrity to be 0.153 ± 0.036 for
367 WT where ± denotes the 95% confidence intervals in the coefficient of variation of OD_{600}
368 as obtained by bootstrapping (**Fig. 7**). These observed fluctuations were significantly
369 higher than the technical noise of 0.086 ± 0.028 (control fluctuations). Technical noise
370 was estimated by performing a similar experiment, but with fluctuations quantified across
371 wells starting with a random population of 10,000 cells rather than a single cell-derived
372 population. Similar to observations in other bacteria, this fluctuation data is consistent
373 with a model of a multi-generation drug-tolerant state in *Klebsiella pneumoniae* that
374 preexists meropenem exposure.

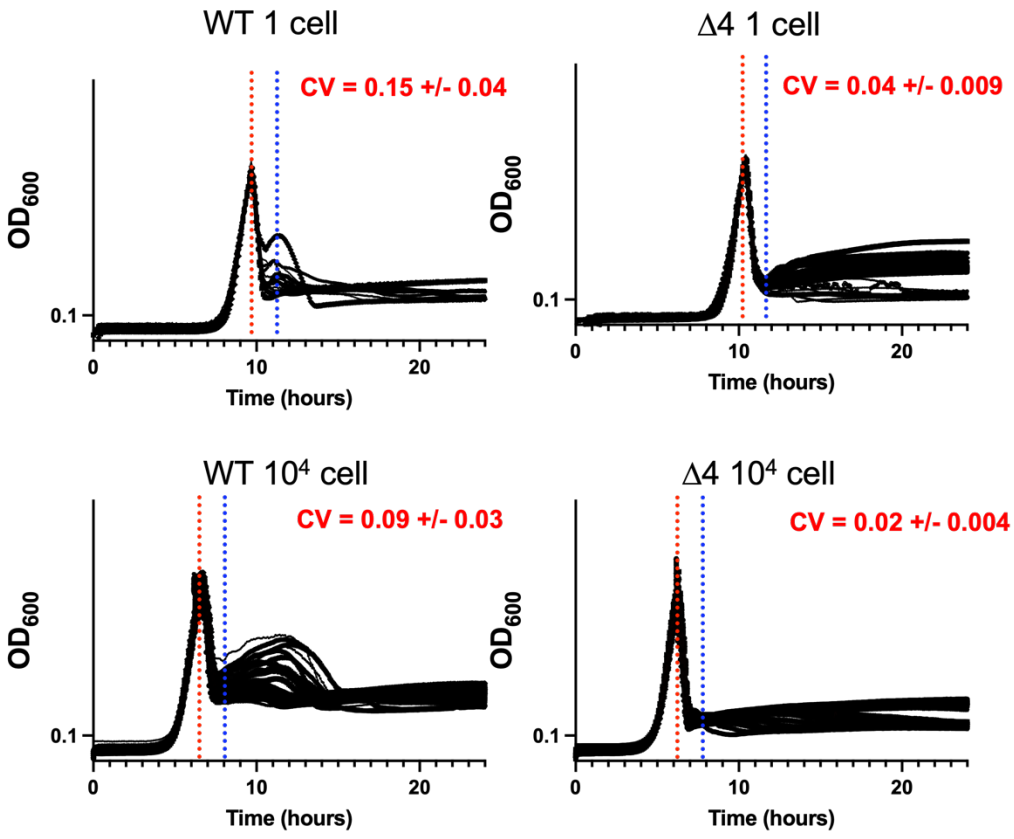

375

376 **Figure 7. Fluctuation test indicates memory in spheroplast population.** Bacteria
377 were diluted to a starting density of 1 cell/well or 10,000 cells/well (control), and grown
378 in a microtiter plate. At OD_{600} =0.3, meropenem (10 µg/mL) was added (red dotted line).

CV (coefficient of variation) calculations were performed at peak killing (blue dotted line).

We hypothesized that the stochasticity originated from variance in background expression of cell envelope stress responses. To test this, we repeated the fluctuation assay in the Δ4 genotype where the observed fluctuations were interestingly much smaller compared to WT with the coefficient of variation being 0.044±0.009, but still significant compared to control fluctuations performed for this strain (**Fig. 7**). The lower value of the observed clonal fluctuations in Δ4 points to faster-switching kinetics, and hence a shorter transient memory of the drug-tolerant state.

Discussion

Infections with Enterobacterales continue to be an active and increasing threat to public health due to their capacity to cause infection, and to gain and disseminate antibiotic resistance genes, with particular risk for vulnerable populations. In this work, we have found that antibiotic tolerance, the ability to sustain viability in the presence of bactericidal antibiotics for extended time periods, is widespread among clinical isolates of Gram-negative pathogens, particularly *Klebsiella pneumoniae*.

To uncover novel factors that modulate β-lactam tolerance in *K. pneumoniae* we performed a genome-wide scan using a TnSeq approach. Because this approach provides a readout of each gene's fitness during a challenge, we were able to identify genes that contribute to meropenem tolerance, and genes that reduce tolerance in *K. pneumoniae*. The screen overall was able to capture several regulatory systems and

individual factors that modulate tolerance along with the internal control PBP1b (a key cell wall synthase required to rebuild the cell wall after catastrophic damage [23]), raising confidence in our approach. This screen also pointed to several well-known and intensely studied cell envelope stress responses that are partly responsible for this strain's ability to undergo the entire process of spheroplast formation, maintenance, and recovery: the Rcs, Pho, Cpx, and OmpR/EnvZ systems.

Interestingly, the OmpR/EnvZ system appears to exert an outsized effect on tolerance. This system is induced by changes in pH and osmolarity, and controls the switch from the larger diameter porin OmpF to the smaller diameter porin OmpC [35]. Formally, it is possible that the porin switch may delay diffusion of meropenem into the cell; however, this is unlikely given that WT and Δ*ompR/envZ* MICs are within essential agreement (**Table S2**). Future work will be directed at delineating the contribution of this system to spheroplast maintenance. Conversely, the Pho and Cpx single system deletion mutants appear to have similar net contributions to meropenem tolerance both in rate of killing and final viability, while still forming detectable spheroplasts capable of recovery. The versatile PhoPQ system senses Mg^{2+} deficiency, presence of antimicrobial peptides, pH and other stresses [36]. Most relevant to the phenotype assayed here, we have previously shown that PhoPQ is required for meropenem tolerance in the related bacterium *Enterobacter cloacae*, via PhoPQ-controlled outer membrane modifications [25]. The Cpx system is a general cell envelope health monitor [37], which controls, among other things, L,D-transpeptidases that may help stabilize the outer membrane [38, 39], and respiratory chain functions [40, 41], which may contribute to ROS production in spheroplasts [17]. Lastly, the Rcs system contributes to meropenem tolerance in a unique

way. Time-dependent killing revealed that viability dropped substantially in the Δ*rcsF* mutant, but this strain's capacity to form spheroplasts and maintain optical density is comparable to the WT parent strain. Interestingly, and consistent with previous work in *E. coli* lysozyme-induced spheroplasts [26], Δ*rcsF* mutant spheroplasts were impaired in their ability to reform successful dividing rods when meropenem is removed. Among other genes, Rcs positively regulates the cell division component *ftsZ* [42], perhaps pointing to a model where upon spheroplast recovery, cell division can commence sooner in WT than in Δ*rcs* cells due to the increased availability of critical divisome components. Taken together, the phenotypes of each individual mutant indicate that aspects of β-lactam tolerance are mediated by distinct response systems, likely with some temporal distinction (**Fig. 7**)

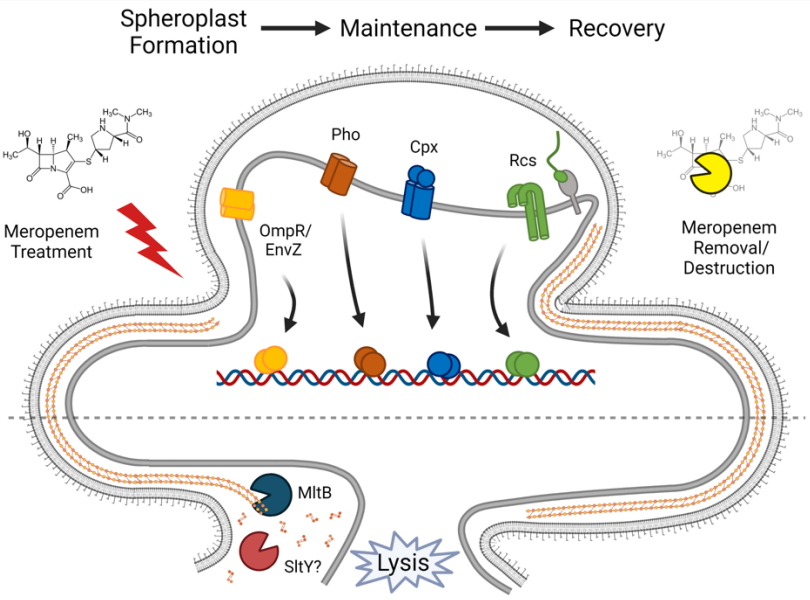

Figure 8: Model of meropenem tolerance as a net result of cell wall degradation and cell envelope stress response induction

Meropenem treatment induces multiple cell envelope stress responses, whose regulons contribute to survival. Lytic transglycosylases MltB and SltY contribute significantly to sacculus degradation, which reduces efficiency of spheroplast recovery.

Because TnSeq has the benefit of also revealing gene disruptions that increase fitness, we simultaneously probed for endogenous factors that reduce meropenem tolerance. *K. pneumoniae* strain TS1's lytic transglycosylase *mltB* answered the screen as a strong candidate that imparts a fitness increase when disrupted. Lytic transglycosylases cleave glycosidic bonds of peptidoglycan strands [24], and have specific and important functions in opportunistic pathogens. For example, in *Acinetobacter baumannii*, *mltB* is a critical factor for pathogenesis by linking complex envelope homeostasis functions with virulence [43]. In *Pseudomonas aeruginosa*, eliminating this enzyme (also in combination with other lytic transglycosylases) increases resistance to cell-wall targeting antibiotics via induction of an endogenous β-lactamase [44, 45]. Disruption of *sltY* and *mltB* in *K. pneumoniae* strain KPNIH1 resulted in 10- 1000 fold increased tolerance to meropenem. Cell morphology around the poles in these mutants was maintained after 24 hours of exposure to meropenem, possibly due to this strain's inability to degrade the old peptidoglycan present when PBPs are inhibited. This maintenance of the cell wall could be what increases survival by preserving the peptidoglycan and envelope-spanning systems, leading to preservation of cell integrity and potentially serving as a scaffold for new cell wall synthesis when meropenem is removed. It is unclear why *mltB* and *sltY* specifically emerge as the only lytic transglycosylases that have this effect on the cell when bacteria generally have multiple

463 redundant lytic transglycosylase paralogs in their genomes; strong phenotypes for single
464 deletion mutants are thus highly unusual.

465 This study presents a deeper insight into β-lactam tolerance and can inform further
466 investigations to understand other aspects of how these dangerous pathogens respond
467 to antibiotics and attain resistance. Attaining an understanding of the detailed workings
468 of this complex phenotype can inform approaches toward finding potential druggable
469 targets to reduce or abolish an organism's capacity for β-lactam tolerance, thus allowing
470 development of novel therapeutics and treatment strategies for tolerant pathogens.

471

472 **Methods**

473 *Culture conditions, tolerance measurement, and complementation*. Unless otherwise
474 stated, all strains were grown in shaking overnight cultures at 37ºC, and tolerance assays
475 were carried out in Brain Heart Infusion (BHI) broth at 37ºC. Tolerance assays were
476 conducted by inoculating overnight culture at a 1:10 ratio into fresh BHI medium
477 containing 10 µg/mL meropenem (TCI, Tokyo, Japan). Cultures were then incubated at
478 37˚C without shaking. Optical density was measured in a VWR V-1200
479 spectrophotometer and viable cells were quantified by serial dilution in BHI medium and
480 spot-titered onto BHI agar. The carbapenemase KPC-2 was purified and added to culture
481 samples at a final concentration of approximately 1 µg/mL prior to serial dilution to
482 deactivate meropenem, thus eliminating meropenem carryover effect.

483

MIC Determination. MICs for all strain backgrounds were determined by diluting overnight cultures 10^7-fold in BHI medium. Diluted cultures were inoculated into BHI containing successive 2-fold concentrations of meropenem in a 96 well microtiter plate at a final volume of 200 µL per well, and incubated at 37°C overnight, leaving one well as an uninoculated control, and one well with cells but without meropenem to ensure growth of the strain. MICs were recorded as the lowest meropenem concentration free from turbidity.

Purification of KPC-2 *enzyme*. The gene for KPC-2 was amplified from the genome of *Enterobacter cloacae* strain 41952, a clinical isolate from WCM, and cloned into the pET21 expression vector. The His-tagged KPC-2 enzyme was overexpressed in BL21 pLysS. A 500 ml culture of LB containing 100 µg/mL ampicillin was induced at OD=0.5 with 1 mM IPTG and incubated shaking at 30°C overnight. The following day, cultures were centrifuged, and pellets were decanted and stored at -80°C until lysis and purification. Pellets were resuspended in resuspension buffer (20 mM Tris, 150 mM NaCl, 5 mM imidazole) and sonicated using the QSonica with the largest tip attachment for 40 minutes total, alternating between 5 second pulses 5 second rests on ice. The lysate was then centrifuged for 45 minutes at 16,000 rpm and the supernatant discarded. In preliminary expression experiments, we found that KPC was mostly in the insoluble fraction. The insoluble pellet was resuspended in binding buffer (20 mM Tris, 150 mM NaCl, 5 mM imidazole, 3 M Urea), and incubated rotating overnight at 4°C to denature and solubilize the KPC-2 protein. The next day, the denatured lysate was centrifuged again at 16,000 rpm for 45 minutes, and the resulting supernatant passed through a

cobalt-charged NTA agarose resin column at room temperature. Six column volumes of wash buffer (20 mM Tris, 150 mM NaCl, 30 mM imidazole, 3 M Urea) were then passed through the column, and the protein eluted in 1.8 mL fractions with increasing concentrations of imidazole in elution buffers (20 mM Tris, 150 mM NaCl, 50-600 mM imidazole, 3 M Urea). Fractions with the highest protein concentrations were pooled, and the total volume was dialyzed into a final storage buffer (20 mM Tris, 150 mM NaCl, 30% glycerol) in three steps, each with decreasing concentrations of imidazole and increasing concentrations of glycerol. Purity was determined by SDS-PAGE, and concentration was estimated with Bio-Rad Bradford Assay kit.

Imaging. All images were taken on a Leica Mdi8 microscope (Leica Microsystems, GmbH, Wetzlar, Germany) with a PECON TempController 2000-1 (Erbach, Germany), heated stage at 37˚C for growth experiments, or room temperature for static images. For timelapse microscopy of spheroplast formation, cells were placed on a 0.8% agarose pad containing BHI and 10 µg/mL meropenem within a gene frame (ThermoFisher, Waltham, MA). For recovery timelapses, KPC-2 enzyme was added at 5 µg/mL to eliminate the meropenem. Frames were taken using autofocus control every five minutes for up to 12 hours. Timelapse video stacks were processed in FIJI (NIH) using the Linear Stack Alignment with SIFT under the Registration plugin (using all default settings with the exception of Expected Transformation, which was changed to Translation) to center cells in the cropped frame. Frame rates were set at 3-4 frames per second for supplemental videos.

Transposon mutagenesis screen and data analysis. *K. pneumoniae* strain TS1 was mutagenized with a Mariner transposon delivered via the *E. coli* donor strain MFD λpir to generate a complex library of kanamycin-resistant transposon mutants. This initial library was frozen as a glycerol stock, and an overnight culture from it was grown in BHI containing kanamycin at 50 µg/mL to form an input library as the comparison for TnSeq analysis. Overnight cultures of this input library were diluted 10-fold into 5 mL BHI containing meropenem (10 ug/mL) and incubated for six hours at 37˚C without shaking, followed by plating on BHI agar plates after treatment with 5 µg/mLKPC-2 enzyme (untreated controls were also generated mirroring the six-hour exposure and recovery populations). Genomic DNA (gDNA) was extracted from all stages of the meropenem challenge and recovery and prepared for Illumina sequencing. Briefly, gDNA extracted from each library was sonicated to generate fragments mostly 200-800 base pairs long which were blunted using NEB Quick Blunting Mix (#E1201L). After blunting, fragments were given A-tails with Taq DNA polymerase to allow ligation of adapter sequences (full lists of primers and reactions can be found in supplemental methods). Ligated fragments were amplified with PCR to enrich transposon-adjacent regions, and then again were PCR amplified with primers to add barcodes, spacer sequences, and Illumina chip attachment ends. The library was run on agarose gel and all fragments 250-600 base pairs were extracted for analysis on the BioAnylazer (Agilent, Santa Clara, CA) to assess before Illumina sequencing. All libraries were sequenced as paired 150 bp reads, though only forward reads were used in the final analysis.

Raw Illumina data were processed in Galaxy using the Cutadapt program to trim reads for length and quality, then mapped with Bowtie2 using the *K. pneumoniae* TS1

553 FASTA reference genome available in NCBI (Biosample accession number
554 SAMN04014921) (full protocol available at this link:
555 https://usegalaxy.org/u/trevorcrossmicro/w/trimming). Mapped reads were analyzed by
556 TnSeq Explorer [46]to calculate insertion density of each gene from each library.
557 Insertion densities were used to calculate an insertion density ratio for each gene from
558 one library to another, thereby comparing essentiality across points in the meropenem
559 challenge. The comparison between library 2 (input) and library 6 (meropenem recovery)
560 was used as the basis for ranking genes in order of essentiality, with genes most essential
561 to meropenem tolerance appearing at the top of the list, while genes which impart a fitness
562 increase when disrupted appearing at the bottom of the list.

563

564 *KPNIH1 validations.* Candidate tolerance genes identified by TnSeq were first validated
565 using an arrayed *K. pneumoniae* KPNIH1 library constructed by the Manoil lab [21].
566 Transposon mutants were grown in 200 µL BHI medium overnight cultures in a 96 well
567 plate. The next day, the overnight culture was diluted 1:10 into BHI containing a final
568 concentration of 10 µg/mL meropenem. At the indicated time points, samples were taken
569 for cfu determination, while simultaneously measuring optical densities in a Spectramax
570 iX3 (Molecular Devices, San Jose, CA) plate reader, and then incubated at 37˚C without
571 shaking for six hours. Final optical density and cfu/mL were recorded and the ratio
572 between final and initial values were calculated to determine the effect of the gene
573 disruption when challenged with meropenem.

574

Strain constructions with pTOX. Strains and oligos are summarized in Table S3. Knock out and reporter strains in *K. pneumoniae* TS1 were constructed using the pTOX5 allelic exchange vector as described in [47]. Briefly, 800-1000 base pair regions flanking regions were amplified using PCR or synthesized de novo and assembled via isothermal assembly into the pTOX SmaI site. Assembled constructs were transformed into DH5α λpir competent cells, plated on LB containing 100 µg/mL chloramphenicol and 1% glucose (LB/CHL/gluc) (to repress the rhamnose inducible toxin gene) and screened for insertion size with primers TC_82 and TC_83, followed by sequence verification through Sanger sequencing. Correct constructs were transformed into conjugal MFD λpir and mated into *K. pneumoniae* TS1 on LB containing 1% glucose and 1.2 mM DAP (LB/gluc/DAP) for 6 hours at 37°C. Transconjugants were isolated back on LB/CHL/gluc and a single colony was grown out in LB containing 1% glucose until the OD reached 0.1-0.2, at which point cells were washed with M9 medium containing 0.2% casamino acids and 1% rhamnose, and plated on solid M9/rham/casamino acids to induce the counterselective toxin and isolate allelic exchange constructs containing the desired modifications. Envelope stress response system deletions were screened using primers flanking the loci of interest and validated using internal primers. Other constructs were validated using primers specific to the modification, or primers flanking the *lac*/Z locus where reporters were inserted.

Miller assay to detect RcsB function and induction. To assess function of the RcsB response regulator, a reporter construct was made by inserting an *rprA-lacZ*$_{MG1655}$ reporter with the *E. coli* MG1655 lacZ gene (abbreviated to *rprA-lacZ*) into the TS1 native *lacZ* locus, eliminating most of the native *lacI* and *lacZ* genes. This construct was

validated first by overexpressing native RcsB on a pBAD plasmid in the presence of 0.2% arabinose on BHI medium from strain TS1 in the reporter background and qualitatively comparing X-gal signal to the construct containing an empty vector. RcsB activation upon meropenem exposure was measured by performing the Miller assay on cell pellets from meropenem-exposed cells at 0, 1, 3, and 6 hours in BHI and control cultures to determine relative units of β-galactosidase activity normalized to cfu/mL of either culture.

Acknowledgements

This work was supported by NIH-NIAID grant R01AI143704 to TD. AS acknowledges support from NIH-NIGMS via grant R35GM148351.

Supplementary Figures

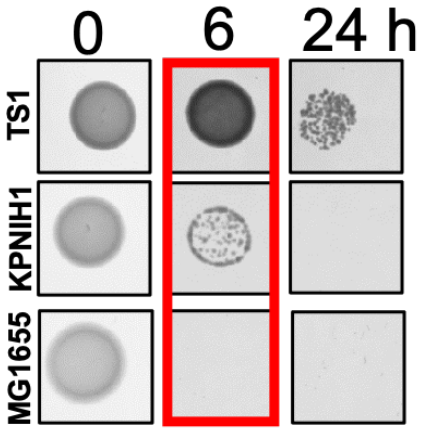

Fig. S1 Tolerance screen validation with benchmark isolates

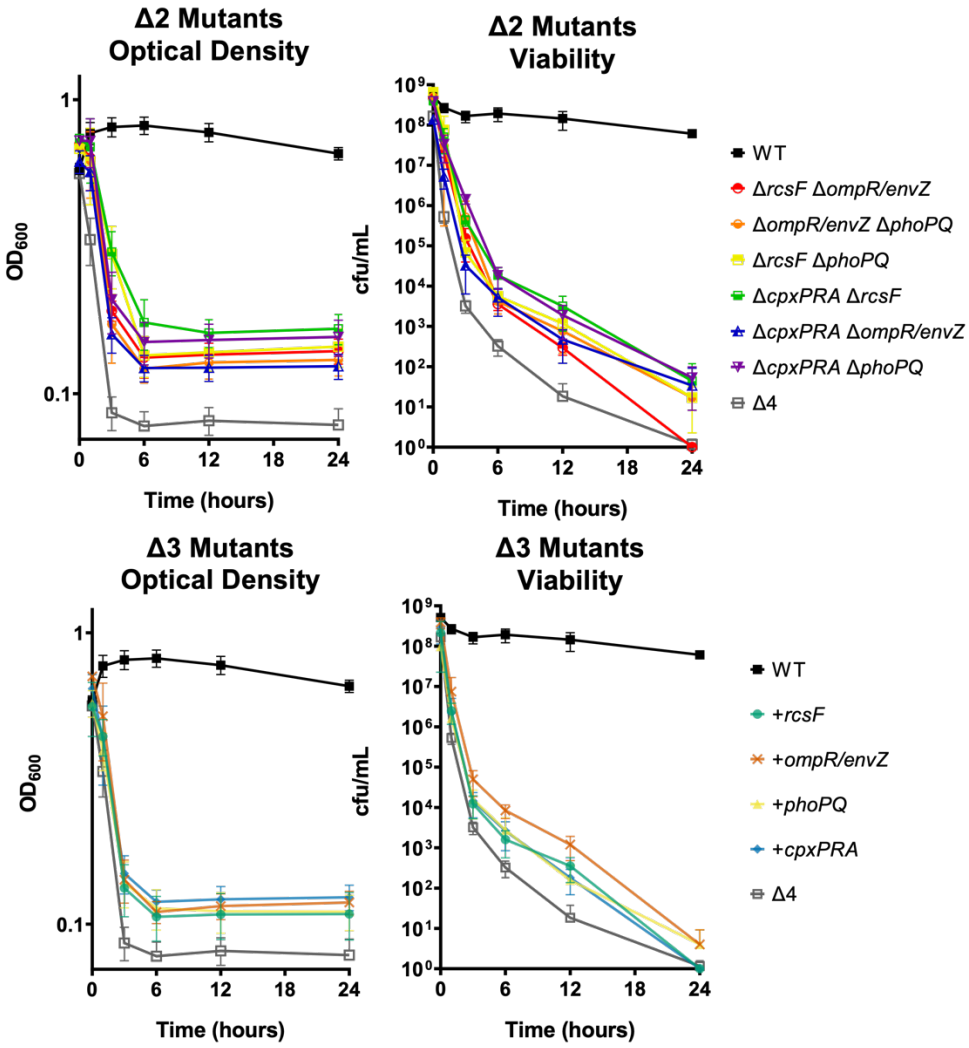

622

623 **Fig. S2 Tolerance phenotypes of CESR mutants**

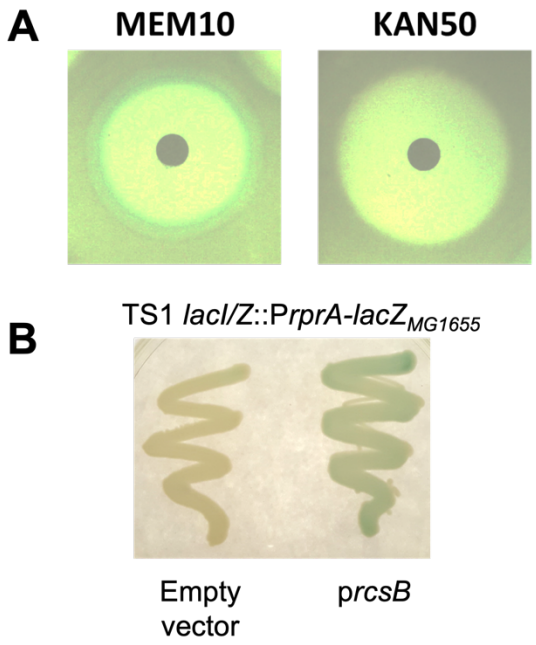

624

625 **Fig. S3 Meropenem induces the Rcs phosphorelay**

626

627 **Supplementary Tables** (preprint version: available upon request

628 tdoerr@cornell.edu)

629 Table S1 – Bloodstream isolate panel with MIC data

Strain	**MIC (µg/mL)** **(n=3 replicates)**
TS1 WT	0.00625
TS1 Δ*rcsF*	0.00625

TS1 Δ*ompR/envZ*	0.003125
TS1 Δ*phoPQ*	0.00625
TS1 Δ*cpxPRA*	0.003125
TS1 Δ*4*	0.001563
KPNIH1 WT	0.05
KPNIH1 *mltB::tn*	0.8
KPNIH1 *sltY::tn*	0.2
MG1655 WT	0.003125

630

631 Table S2 – MICs of strains constructed in this study

632 Table S3 – Strains and Oligos

633 Table S4 – TnSeq hits raw data

634

635

636

637

References:

1. Miller WR, Arias CA. ESKAPE pathogens: antimicrobial resistance, epidemiology, clinical impact and therapeutics. Nat Rev Microbiol. 2024;22(10):598-616. Epub 2024/06/04. doi: 10.1038/s41579-024-01054-w. PubMed PMID: 38831030.
2. Haney EF, Hancock REW. Addressing Antibiotic Failure—Beyond Genetically Encoded Antimicrobial Resistance. Frontiers in Drug Discovery. 2022;2. doi: 10.3389/fddsv.2022.892975.
3. Balaban NQ, Helaine S, Lewis K, Ackermann M, Aldridge B, Andersson DI, et al. Definitions and guidelines for research on antibiotic persistence. Nat Rev Microbiol. 2019;17(7):441-8. Epub 2019/04/14. doi: 10.1038/s41579-019-0196-3. PubMed PMID: 30980069; PubMed Central PMCID: PMCPMC7136161.
4. Roberts D, Higgs E, Rutman a, Cole P. Isolation of spheroplastic forms of Haemophilus influenzae from sputum in conventionally treated chronic bronchial sepsis using selective medium supplemented with N-acetyl-D-glucosamine: possible reservoir for re-emergence of infection. British medical journal (Clinical research ed). 1984;289:1409-12. doi: 10.1016/j.compmedimag.2005.07.001. PubMed PMID: 6437576.
5. Monahan LG, Turnbull L, Osvath SR, Birch D, Charles IG, Whitchurch CB. Rapid conversion of Pseudomonas aeruginosa to a spherical cell morphotype facilitates tolerance to carbapenems and penicillins but increases susceptibility to antimicrobial peptides. Antimicrob Agents Chemother. 2014;58(4):1956-62. doi: 10.1128/AAC.01901-13. PubMed PMID: 24419348; PubMed Central PMCID: PMCPMC4023726.
6. Dörr T, Davis BM, Waldor MK. Endopeptidase-mediated beta lactam tolerance. PLoS Pathog. 2015;11(4):e1004850. doi: 10.1371/journal.ppat.1004850. PubMed PMID: 25884840; PubMed Central PMCID: PMCPMC4401780.
7. Cross T, Ransegnola B, Shin JH, Weaver A, Fauntleroy K, VanNieuwenhze MS, et al. Spheroplast-Mediated Carbapenem Tolerance in Gram-Negative Pathogens. Antimicrob Agents Chemother. 2019;63(9). doi: 10.1128/AAC.00756-19. PubMed PMID: 31285232; PubMed Central PMCID: PMCPMC6709500.
8. Mickiewicz KM, Kawai Y, Drage L, Gomes MC, Davison F, Pickard R, et al. Possible role of L-form switching in recurrent urinary tract infection. Nat Commun. 2019;10(1):4379. Epub 2019/09/29. doi: 10.1038/s41467-019-12359-3. PubMed PMID: 31558767; PubMed Central PMCID: PMCPMC6763468.
9. Claessen D, Errington J. Cell Wall Deficiency as a Coping Strategy for Stress. Trends Microbiol. 2019;27(12):1025-33. Epub 2019/08/20. doi: 10.1016/j.tim.2019.07.008. PubMed PMID: 31420127.
10. Errington J. Cell wall-deficient, L-form bacteria in the 21st century: a personal perspective. Biochemical Society Transactions. 2017;45:287-95. doi: 10.1042/BST20160435. PubMed PMID: 28408469.
11. Paczosa MK, Mecsas J. Klebsiella pneumoniae: Going on the Offense with a Strong Defense. Microbiol Mol Biol Rev. 2016;80(3):629-61. Epub 2016/06/17. doi: 10.1128/mmbr.00078-15. PubMed PMID: 27307579; PubMed Central PMCID: PMCPMC4981674.
12. Murray CJL, Ikuta KS, Sharara F, Swetschinski L, Robles Aguilar G, Gray A, et al. Global burden of bacterial antimicrobial resistance in 2019: a systematic analysis. The Lancet. 2022;399(10325):629-55. doi: 10.1016/S0140-6736(21)02724-0.
13. Chen TA, Chuang YT, Lin CH. A Decade-Long Review of the Virulence, Resistance, and Epidemiological Risks of Klebsiella pneumoniae in ICUs. Microorganisms. 2024;12(12). Epub 2025/01/08. doi: 10.3390/microorganisms12122548. PubMed PMID: 39770751; PubMed Central PMCID: PMCPMC11678397.

14. Dörr T. Understanding tolerance to cell wall–active antibiotics. Annals of the New York Academy of Sciences. 2021;1496(1):35-58. doi: https://doi.org/10.1111/nyas.14541.
15. Cho H, Uehara T, Bernhardt TG. Beta-lactam antibiotics induce a lethal malfunctioning of the bacterial cell wall synthesis machinery. Cell. 2014;159(6):1300-11. doi: 10.1016/j.cell.2014.11.017. PubMed PMID: 25480295; PubMed Central PMCID: PMCPMC4258230.
16. Lobritz MA, Andrews IW, Braff D, Porter CBM, Gutierrez A, Furuta Y, et al. Increased energy demand from anabolic-catabolic processes drives β-lactam antibiotic lethality. Cell Chem Biol. 2022;29(2):276-86.e4. Epub 2022/01/07. doi: 10.1016/j.chembiol.2021.12.010. PubMed PMID: 34990601; PubMed Central PMCID: PMCPMC8857051.
17. Shin JH, Choe D, Ransegnola B, Hong HR, Onyekwere I, Cross T, et al. A multifaceted cellular damage repair and prevention pathway promotes high-level tolerance to beta-lactam antibiotics. EMBO Rep. 2021:e51790. Epub 2021/01/20. doi: 10.15252/embr.202051790. PubMed PMID: 33463026.
18. Held K, Gasper J, Morgan S, Siehnel R, Singh P, Manoil C. Determinants of Extreme beta-Lactam Tolerance in the Burkholderia pseudomallei Complex. Antimicrob Agents Chemother. 2018;62(4). doi: 10.1128/AAC.00068-18. PubMed PMID: 29439964; PubMed Central PMCID: PMCPMC5913950.
19. Dörr T, Alvarez L, Delgado F, Davis BM, Cava F, Waldor MK. A cell wall damage response mediated by a sensor kinase/response regulator pair enables beta-lactam tolerance. Proc Natl Acad Sci U S A. 2016;113(2):404-9. doi: 10.1073/pnas.1520333113. PubMed PMID: 26712007; PubMed Central PMCID: PMCPMC4720315.
20. Gefen O, Chekol B, Strahilevitz J, Balaban NQ. TDtest: easy detection of bacterial tolerance and persistence in clinical isolates by a modified disk-diffusion assay. Sci Rep. 2017;7:41284. doi: 10.1038/srep41284. PubMed PMID: 28145464; PubMed Central PMCID: PMCPMC5286521 financial interests in this work.
21. Ramage B, Erolin R, Held K, Gasper J, Weiss E, Brittnacher M, et al. Comprehensive Arrayed Transposon Mutant Library of Klebsiella pneumoniae Outbreak Strain KPNIH1. J Bacteriol. 2017;199(20). doi: 10.1128/JB.00352-17. PubMed PMID: 28760848; PubMed Central PMCID: PMCPMC5637181.
22. Weaver AI, Murphy SG, Umans B, Tallavajhala S, Onyekwere I, Wittels S, et al. Genetic determinants of penicillin tolerance in Vibrio cholerae. Antimicrob Agents Chemother. 2018. doi: 10.1128/AAC.01326-18. PubMed PMID: 30061291.
23. Ranjit DK, Jorgenson MA, Young KD. PBP1B Glycosyltransferase and Transpeptidase Activities Play Different Essential Roles during the De Novo Regeneration of Rod Morphology in Escherichia coli. J Bacteriol. 2017;199(7). Epub 2017/01/18. doi: 10.1128/jb.00612-16. PubMed PMID: 28096447; PubMed Central PMCID: PMCPMC5350282.
24. Weaver A, Taguchi A, Dörr T. Masters of Misdirection: Peptidoglycan Glycosidases in Bacterial Growth. J Bacteriol. 2023;205(3):e0042822. Epub 2023/02/10. doi: 10.1128/jb.00428-22. PubMed PMID: 36757204; PubMed Central PMCID: PMCPMC10029718.
25. Murtha AN, Kazi MI, Schargel RD, Cross T, Fihn C, Cattoir V, et al. High-level carbapenem tolerance requires antibiotic-induced outer membrane modifications. PLoS Pathog. 2022;18(2):e1010307. Epub 20220207. doi: 10.1371/journal.ppat.1010307. PubMed PMID: 35130322; PubMed Central PMCID: PMCPMC8853513.
26. Ranjit DK, Young KD. The Rcs stress response and accessory envelope proteins are required for de novo generation of cell shape in Escherichia coli. J Bacteriol. 2013;195(11):2452-62. Epub 2013/04/02. doi: 10.1128/JB.00160-13. PubMed PMID: 23543719; PubMed Central PMCID: PMCPMC3676047.
27. Laubacher ME, Ades SE. The Rcs phosphorelay is a cell envelope stress response activated by peptidoglycan stress and contributes to intrinsic antibiotic resistance. J Bacteriol.

2008;190(6):2065-74. doi: 10.1128/JB.01740-07. PubMed PMID: 18192383; PubMed Central PMCID: PMCPMC2258881.

28. Rousseau CJ, Fraikin N, Zedek S, Van Melderen L. Are envelope stress responses essential for persistence to β-lactams in Escherichia coli? Antimicrob Agents Chemother. 2023;67(10):e0032923. Epub 2023/10/03. doi: 10.1128/aac.00329-23. PubMed PMID: 37787525; PubMed Central PMCID: PMCPMC10583663.

29. Wall E, Majdalani N, Gottesman S. The Complex Rcs Regulatory Cascade. Annu Rev Microbiol. 2018;72:111-39. doi: 10.1146/annurev-micro-090817-062640. PubMed PMID: 29897834.

30. Harmange G, Hueros RAR, Schaff DL, Emert B, Saint-Antoine M, Kim LC, et al. Disrupting cellular memory to overcome drug resistance. Nature Communications. 2023;14(1):7130. doi: 10.1038/s41467-023-41811-8.

31. Shaffer SM, Dunagin MC, Torborg SR, Torre EA, Emert B, Krepler C, et al. Rare cell variability and drug-induced reprogramming as a mode of cancer drug resistance. Nature. 2017;546(7658):431-5. doi: 10.1038/nature22794.

32. Singh A, Saint-Antoine M. Probing transient memory of cellular states using single-cell lineages. Frontiers in Microbiology. 2023;13. doi: 10.3389/fmicb.2022.1050516.

33. Hossain T, Singh A, Butzin NC. Escherichia coli cells are primed for survival before lethal antibiotic stress. Microbiology Spectrum. 2023;11(5):e01219-23. doi: doi:10.1128/spectrum.01219-23.

34. Guha M, Singh A, Butzin NC. Gram-positive bacteria are primed for surviving lethal doses of antibiotics and chemical stress. bioRxiv. 2024:2024.05.28.596288. doi: 10.1101/2024.05.28.596288.

35. Kenney LJ, Anand GS. EnvZ/OmpR Two-Component Signaling: An Archetype System That Can Function Noncanonically. EcoSal Plus. 2020;9(1). Epub 2020/02/01. doi: 10.1128/ecosalplus.ESP-0001-2019. PubMed PMID: 32003321; PubMed Central PMCID: PMCPMC7192543.

36. Groisman EA, Duprey A, Choi J. How the PhoP/PhoQ System Controls Virulence and Mg(2+) Homeostasis: Lessons in Signal Transduction, Pathogenesis, Physiology, and Evolution. Microbiol Mol Biol Rev. 2021;85(3):e0017620. Epub 2021/07/01. doi: 10.1128/mmbr.00176-20. PubMed PMID: 34191587; PubMed Central PMCID: PMCPMC8483708.

37. Raivio TL. Everything old is new again: an update on current research on the Cpx envelope stress response. Biochim Biophys Acta. 2014;1843(8):1529-41. Epub 2013/11/05. doi: 10.1016/j.bbamcr.2013.10.018. PubMed PMID: 24184210.

38. Morè N, Martorana AM, Biboy J, Otten C, Winkle M, Serrano CKG, et al. Peptidoglycan Remodeling Enables Escherichia coli To Survive Severe Outer Membrane Assembly Defect. mBio. 2019;10(1). Epub 2019/02/07. doi: 10.1128/mBio.02729-18. PubMed PMID: 30723128; PubMed Central PMCID: PMCPMC6428754.

39. Bernal-Cabas M, Ayala JA, Raivio TL. The Cpx envelope stress response modifies peptidoglycan cross-linking via the L,D-transpeptidase LdtD and the novel protein YgaU. J Bacteriol. 2015;197(3):603-14. Epub 2014/11/26. doi: 10.1128/jb.02449-14. PubMed PMID: 25422305; PubMed Central PMCID: PMCPMC4285979.

40. Guest RL, Wang J, Wong JL, Raivio TL. A Bacterial Stress Response Regulates Respiratory Protein Complexes To Control Envelope Stress Adaptation. J Bacteriol. 2017;199(20). Epub 2017/08/02. doi: 10.1128/jb.00153-17. PubMed PMID: 28760851; PubMed Central PMCID: PMCPMC5637174.

41. Tsviklist V, Guest RL, Raivio TL. The Cpx Stress Response Regulates Turnover of Respiratory Chain Proteins at the Inner Membrane of Escherichia coli. Front Microbiol. 2021;12:732288. Epub 2022/02/15. doi: 10.3389/fmicb.2021.732288. PubMed PMID: 35154019; PubMed Central PMCID: PMCPMC8831704.

42. Carballès F, Bertrand C, Bouché JP, Cam K. Regulation of Escherichia coli cell division genes ftsA and ftsZ by the two-component system rcsC-rcsB. Mol Microbiol. 1999;34(3):442-50. Epub 1999/11/17. doi: 10.1046/j.1365-2958.1999.01605.x. PubMed PMID: 10564486.

43. Crépin S, Ottosen EN, Peters K, Smith SN, Himpsl SD, Vollmer W, et al. The lytic transglycosylase MltB connects membrane homeostasis and in vivo fitness of Acinetobacter baumannii. Mol Microbiol. 2018;109(6):745-62. Epub 2018/06/10. doi: 10.1111/mmi.14000. PubMed PMID: 29884996; PubMed Central PMCID: PMCPMC6185781.

44. Cavallari JF, Lamers RP, Scheurwater EM, Matos AL, Burrows LL. Changes to its peptidoglycan-remodeling enzyme repertoire modulate β-lactam resistance in Pseudomonas aeruginosa. Antimicrob Agents Chemother. 2013;57(7):3078-84. Epub 2013/04/25. doi: 10.1128/aac.00268-13. PubMed PMID: 23612194; PubMed Central PMCID: PMCPMC3697359.

45. Lamers RP, Nguyen UT, Nguyen Y, Buensuceso RN, Burrows LL. Loss of membrane-bound lytic transglycosylases increases outer membrane permeability and β-lactam sensitivity in Pseudomonas aeruginosa. Microbiologyopen. 2015;4(6):879-95. Epub 2015/09/17. doi: 10.1002/mbo3.286. PubMed PMID: 26374494; PubMed Central PMCID: PMCPMC4694138.

46. Solaimanpour S, Sarmiento F, Mrázek J. Tn-Seq Explorer: A Tool for Analysis of High-Throughput Sequencing Data of Transposon Mutant Libraries. PLOS ONE. 2015;10(5):e0126070. doi: 10.1371/journal.pone.0126070.

47. Lazarus JE, Warr AR, Kuehl CJ, Giorgio RT, Davis BM, Waldor MK. A New Suite of Allelic-Exchange Vectors for the Scarless Modification of Proteobacterial Genomes. Appl Environ Microbiol. 2019;85(16). Epub 2019/06/16. doi: 10.1128/aem.00990-19. PubMed PMID: 31201277; PubMed Central PMCID: PMCPMC6677854.